H1prelim-04-072

Measurement of $F_2^{c\bar{c}}$ and $F_2^{b\bar{b}}$ at High Q^2

H1 Collaboration

Abstract

A measurement is presented of the charm and beauty cross sections at for $Q^2 > 150$ GeV and $0.1 < y < 0.7$, using a method based on the distance of closest approach of tracks, reconstructed using the central silicon tracker, to the production vertex. The data are divided into 3 x-Q^2 bins and values for $F_2^{c\bar{c}}$ and $F_2^{b\bar{b}}$ are evaluated.

Prepared for DIS 2004, Strbske Pleso, Slovakia

Cross sections for $Q^2 > 150\ \mathrm{GeV}^2$, $0.1 < y < 0.7$:

$$\sigma_{c\bar{c}} = 431 \pm 59 \pm 69\ \mathrm{pb}$$

$$\sigma_{b\bar{b}} = 45 \pm 11 \pm 11\ \mathrm{pb}$$

Compared with results of a next to leading order QCD fit which was fitted to inclusive cross sections from H1 [1]:

$$\sigma_{c\bar{c}} = 455\ \mathrm{pb}$$

$$\sigma_{b\bar{b}} = 51.8\ \mathrm{pb}$$

References

[1] C. Adloff *et al.* [H1 Collaboration], Eur. Phys. J **C 30** (2003) 1-32 [hep-ex/0304003].

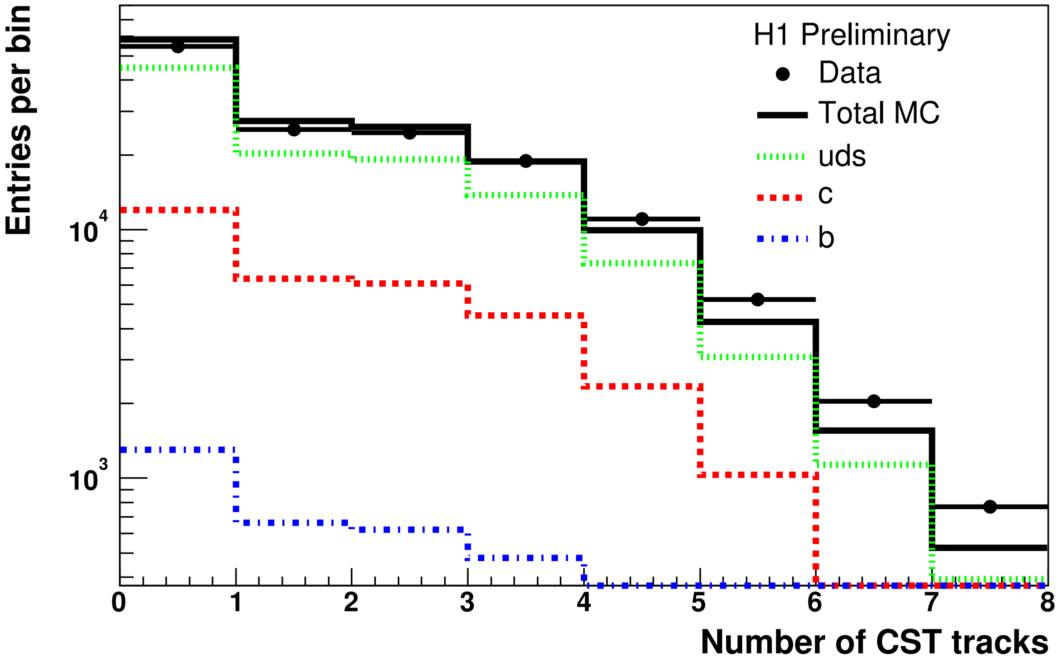

Figure 1: The number of reconstructed central silicon tracker (CST) tracks per jet (or per event if there are no jets with $P_T > 5$ GeV). Each CST track is required to have at least 2 CST hits and $P_T > 0.5$ GeV. Also included is the expectation from the RAPGAP Monte Carlo, showing the contribution from the various quark flavours after applying the scale factors obtained from the fit of the significance distributions of the data (see figure 10).

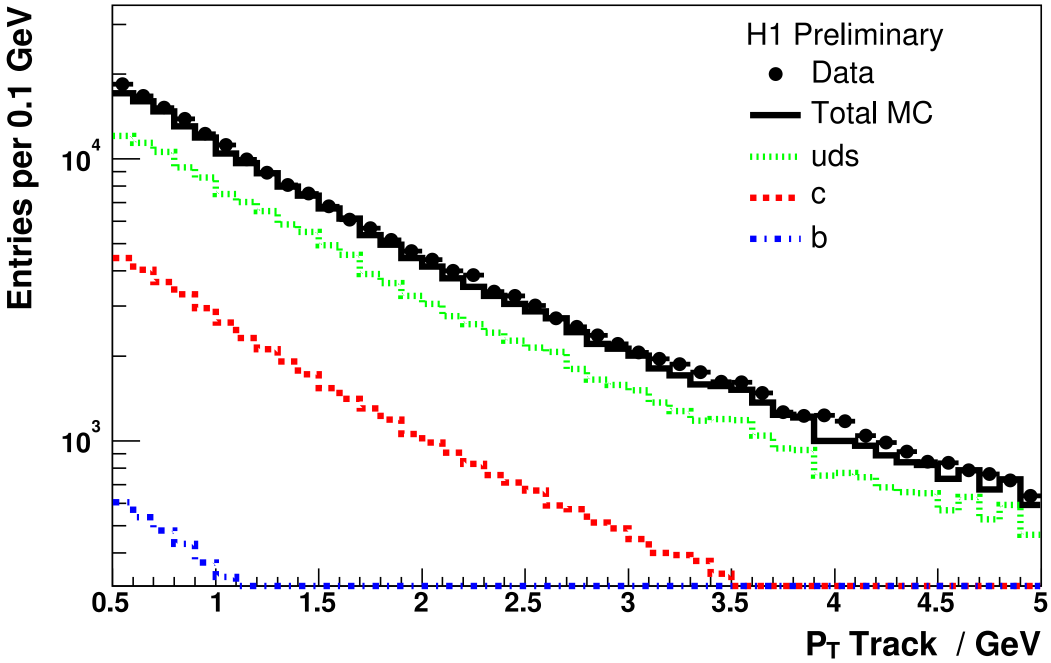

Figure 2: The transverse momentum distribution of all CST tracks. Also included is the expectation from the RAPGAP Monte Carlo, showing the contribution from the various quark flavours after applying the scale factors obtained from the fit to the significance distributions of the data.

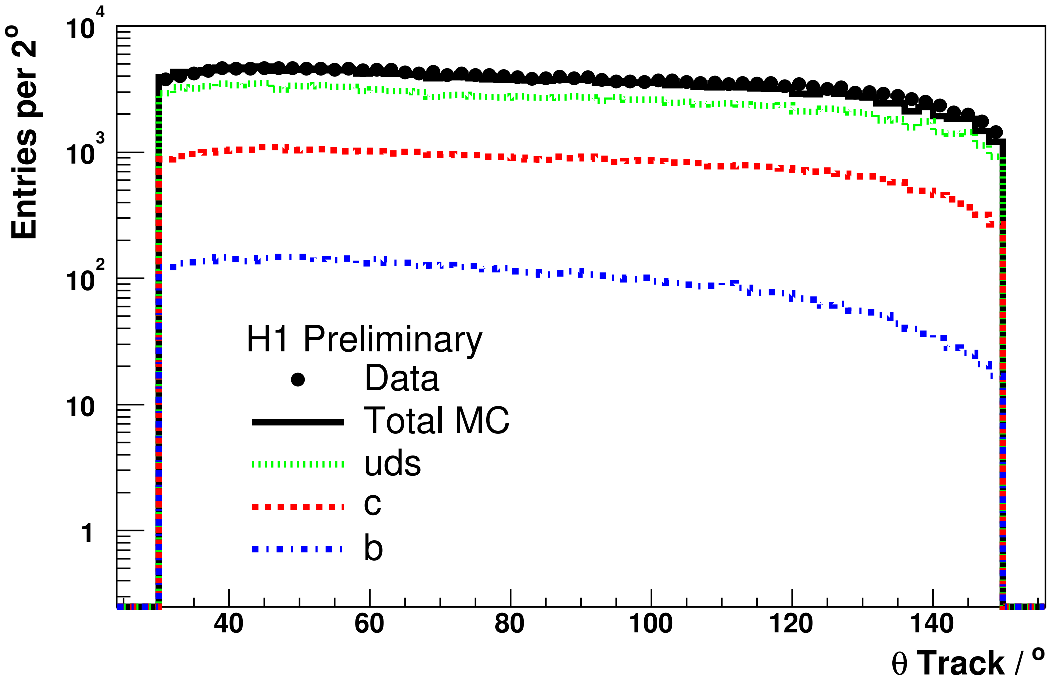

Figure 3: The theta distribution of all CST tracks. Also included is the expectation from the RAPGAP Monte Carlo, showing the contribution from the various quark flavours after applying the scale factors obtained from the fit to the significance distributions of the data.

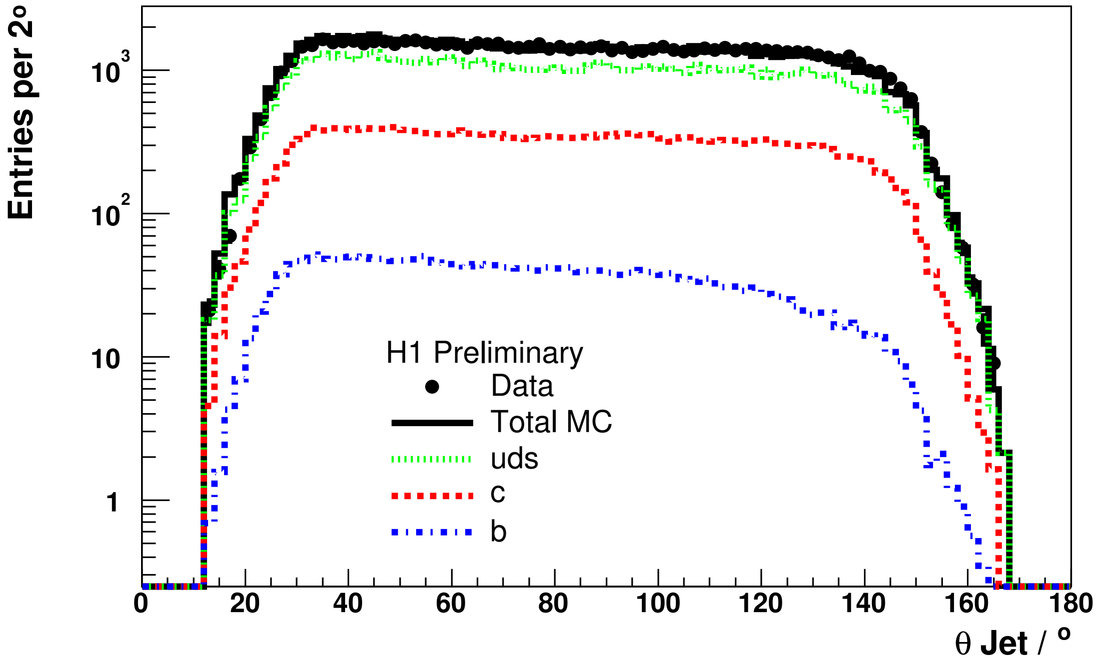

Figure 4: The theta distribution of all jets which contain at least 1 reconstructed CST track within a cone of radius 1.0. Also included is the expectation from the RAPGAP Monte Carlo after applying the scale factors obtained from the fit to the significance distributions of the data.

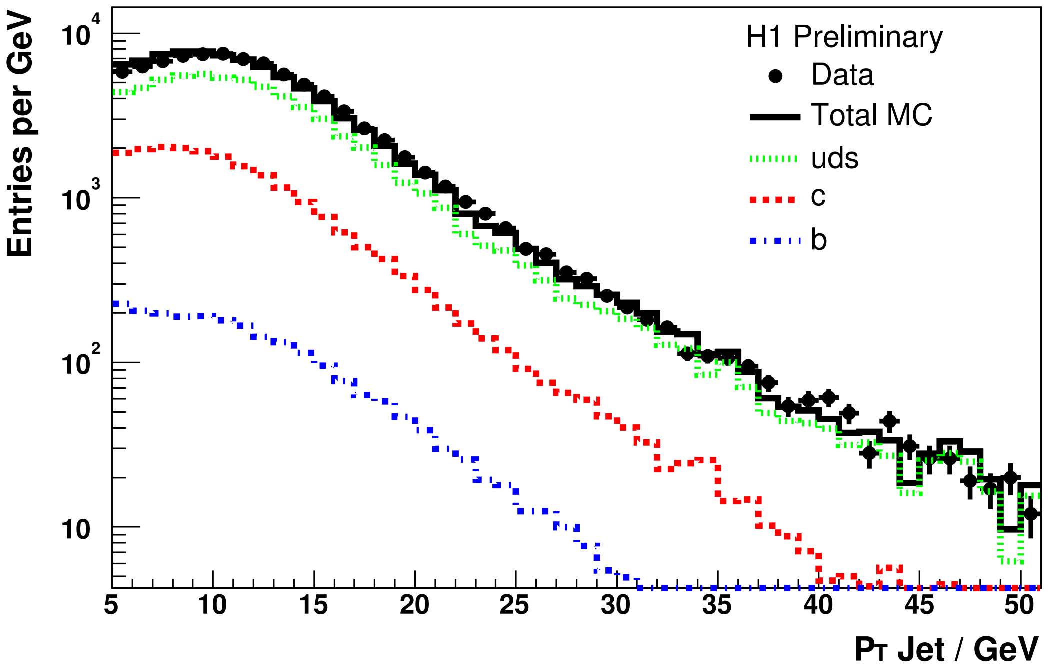

Figure 5: The transverse momentum distribution of all jets which contain at least 1 reconstructed CST track within a cone of radius 1.0. If there are no reconstructed jets the complete hadronic final state P_T is used. Also included is the expectation from the RAPGAP Monte Carlo, showing the contribution from the various quark flavours after applying the scale factors obtained from the fit to the significance distributions of the data.

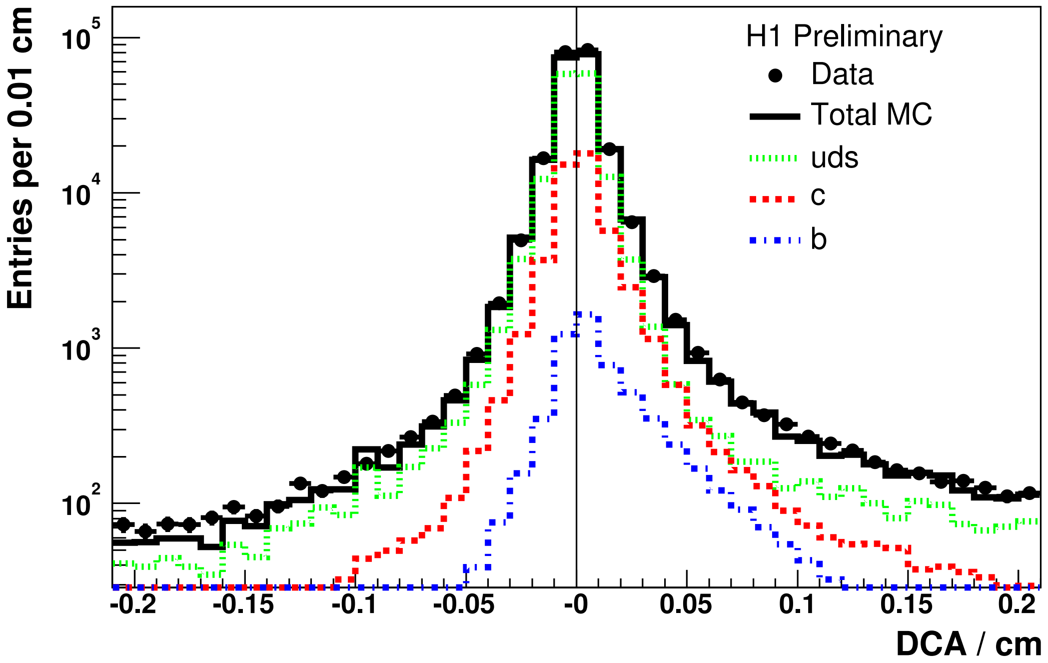

Figure 6: The distance of closest approach of a track to the vertex (DCA) in the XY plane for all CST tracks. Also included is the expectation from the RAPGAP Monte Carlo, showing the contribution from the various quark flavours after applying the scale factors obtained from the fit to the significance distributions of the data.

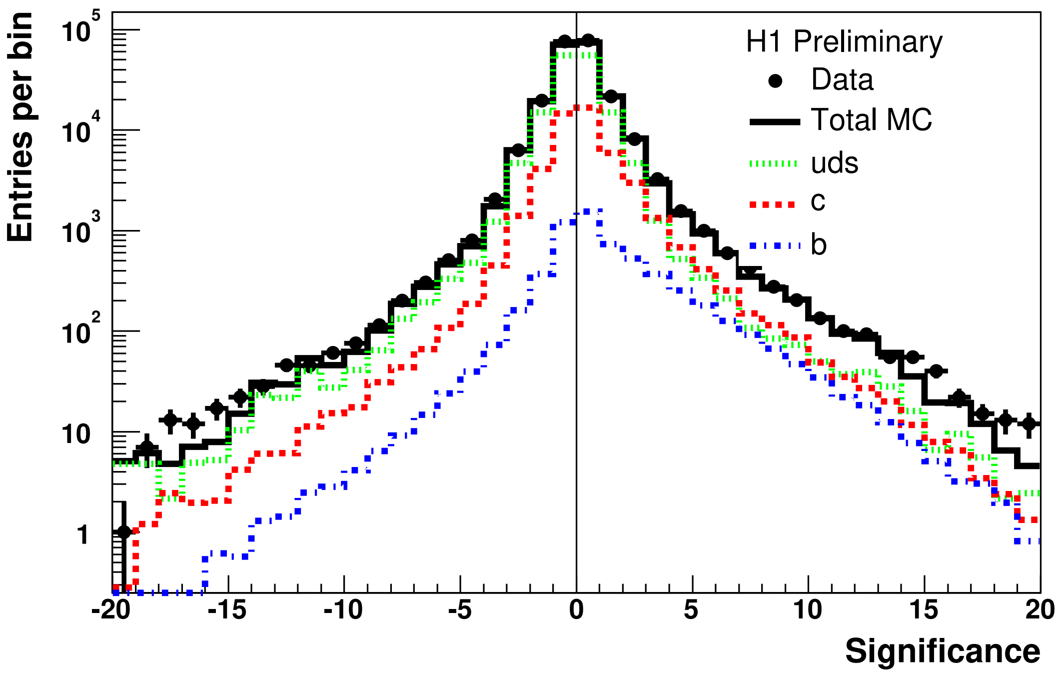

Figure 7: The signed significance ($DCA/\sigma(DCA)$ distribution for all CST tracks, where $\sigma(DCA)$ is the error on the DCA. The sign is defined as positive (negative) if the azimuthal difference between the jet-axis and the vector between the vertex and the point of closest approach of the track is less (greater) than 90°. If there are no reconstructed jets in the event the azimuthal difference is taken with respect to the complete hadronic final state. Also included is the expectation from the RAPGAP Monte Carlo, showing the contribution from the various quark flavours after applying the scale factors obtained from the fit to the significance distributions of the data.

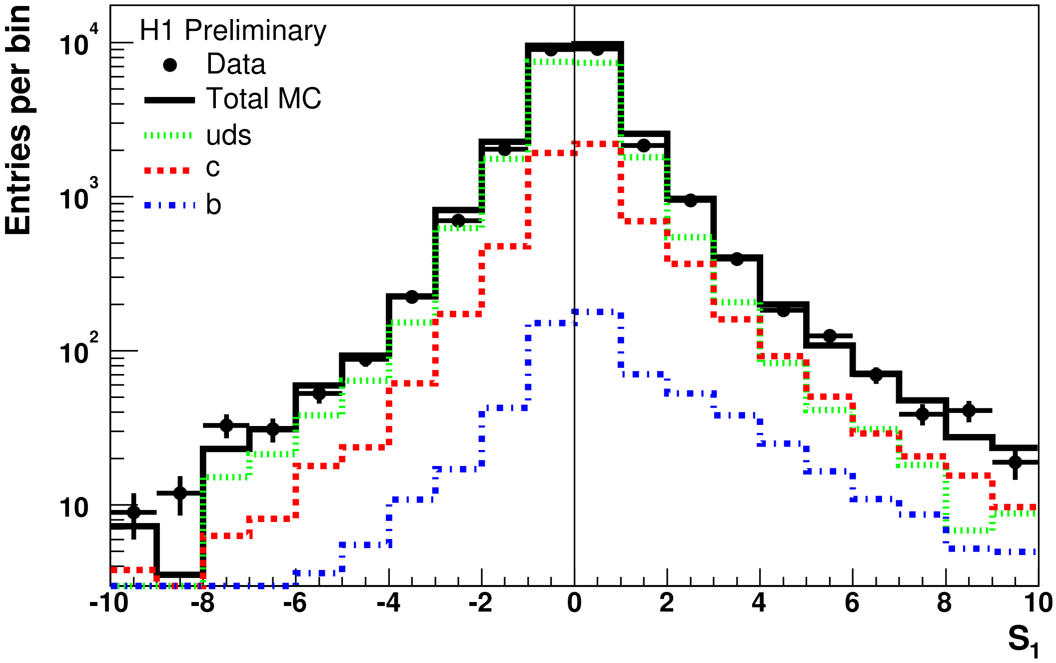

Figure 8: The signed significance $S_1 = DCA/\sigma(DCA)$ distribution for all jets that contain 1 reconstructed CST track. Also included is the expectation from the RAPGAP Monte Carlo, showing the contribution from the various quark flavours after applying the scale factors obtained from the fit to the significance distributions of the data.

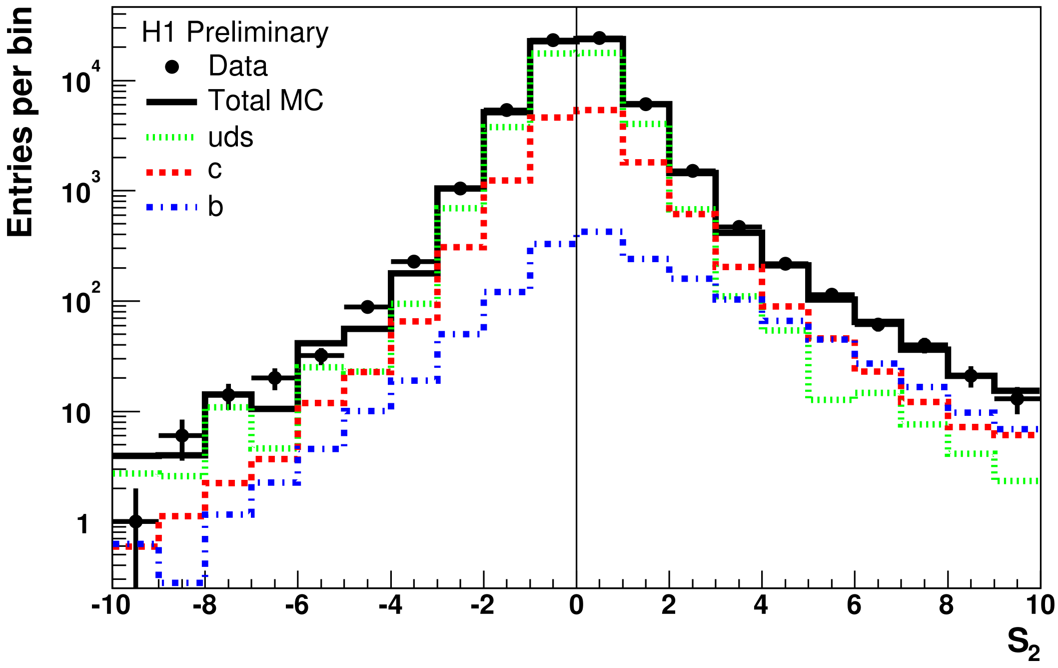

Figure 9: The signed significance $S_2 = DCA/\sigma(DCA)$ distribution of the track with the second largest absolute value of significance for all jets that contain 2 or more reconstructed CST tracks. Also included is the expectation from the RAPGAP Monte Carlo, showing the contribution from the various quark flavours after applying the scale factors obtained from the fit to the significance distributions of the data.

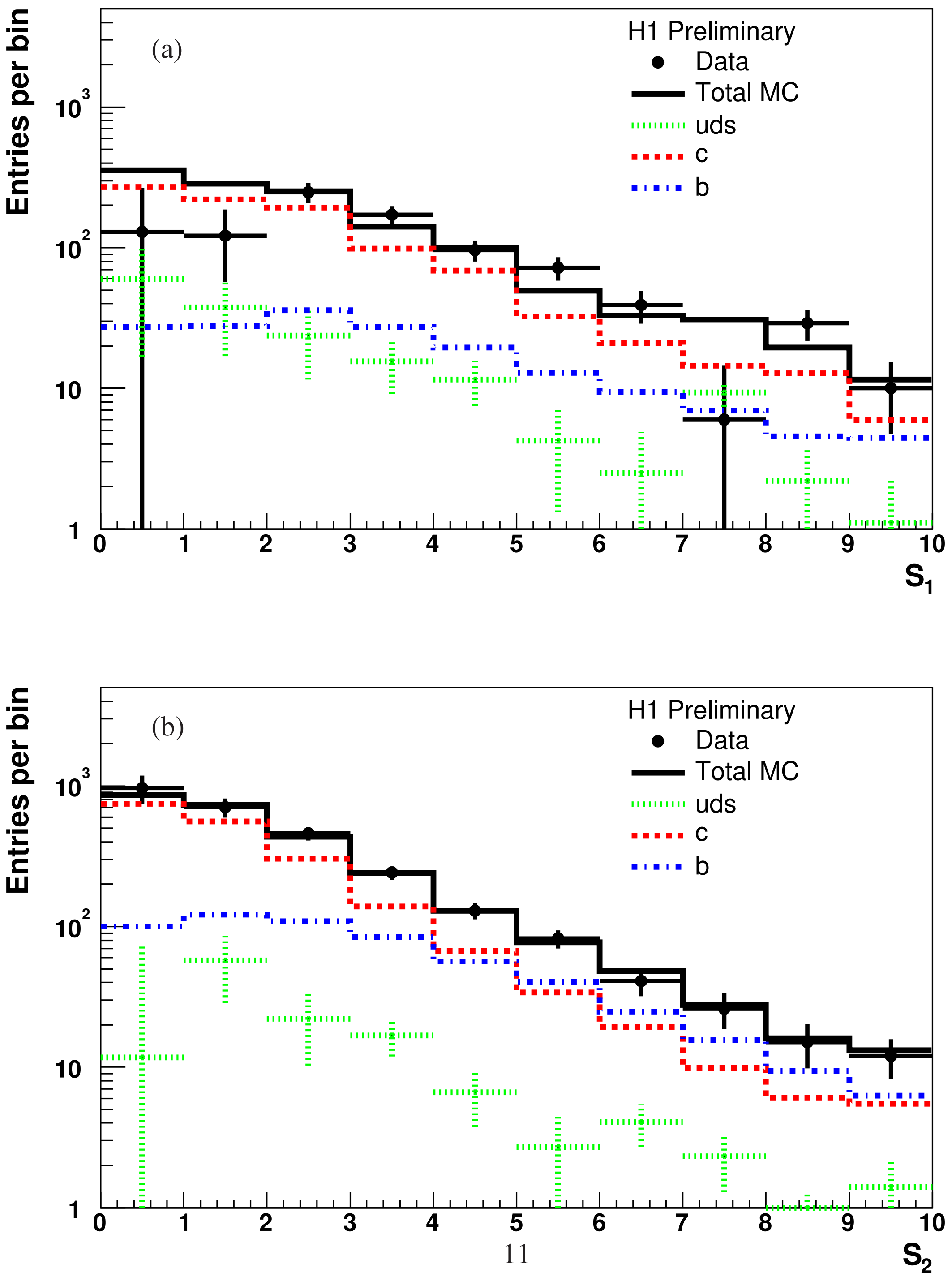

Figure 10: The distibutions (a) S_1 and (b) S_2, after subtracting the bins with equal magnitude but negative sign from the postive. Also included is the results from the fit to the data of the Monte Carlo distributions of events arising from c quarks or b quarks. The light quark constribution is also shown.

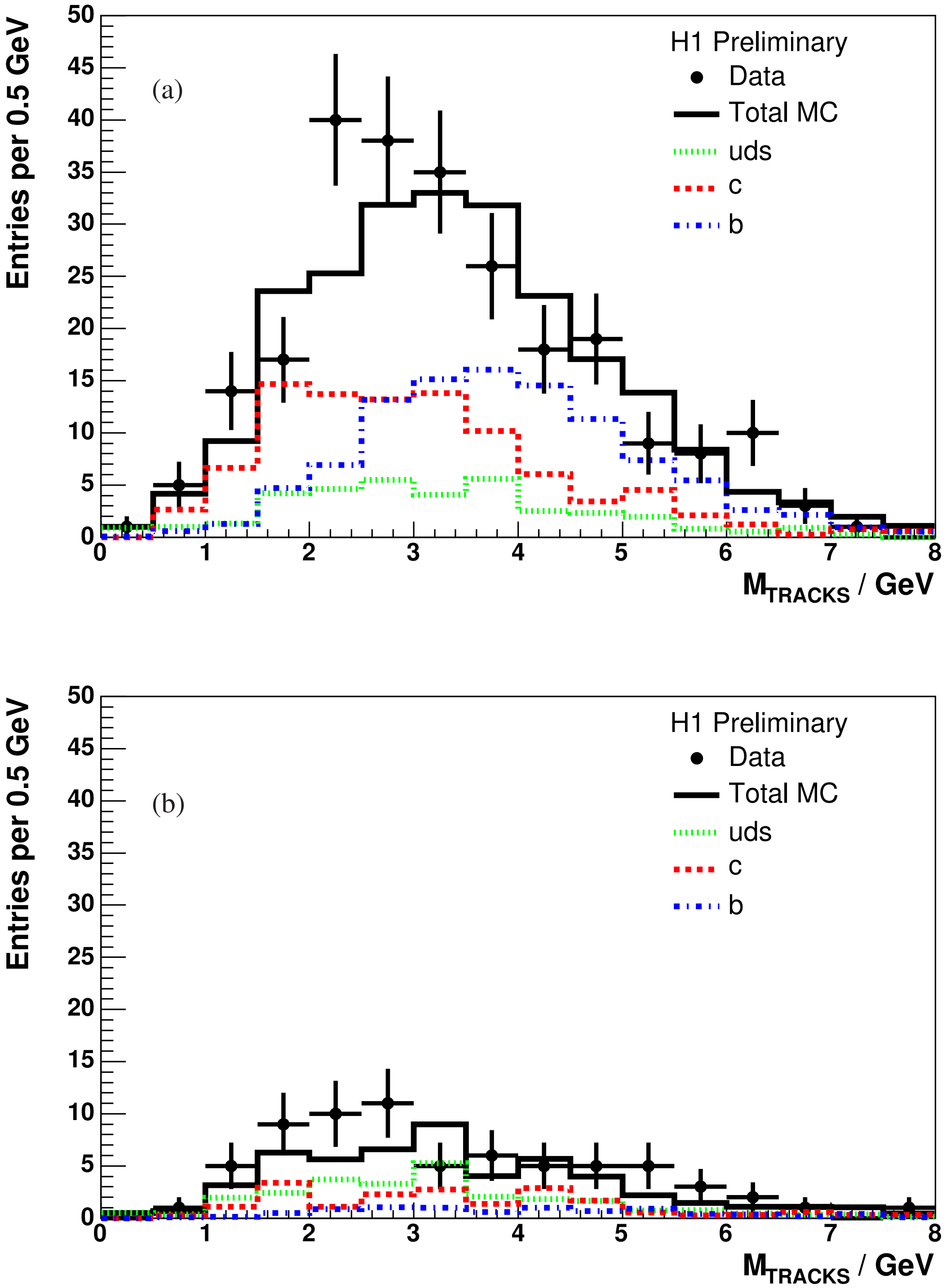

Figure 11: The invariant mass distribution of all track in jets for which (a) $5 < S_2 < 10$ and (b) $-10 < S_2 < -5$. Also included is the expectation from the RAPGAP Monte Carlo, showing the contribution from the various quark flavours after applying the scale factors obtained from the fit to the significance distributions of the data.

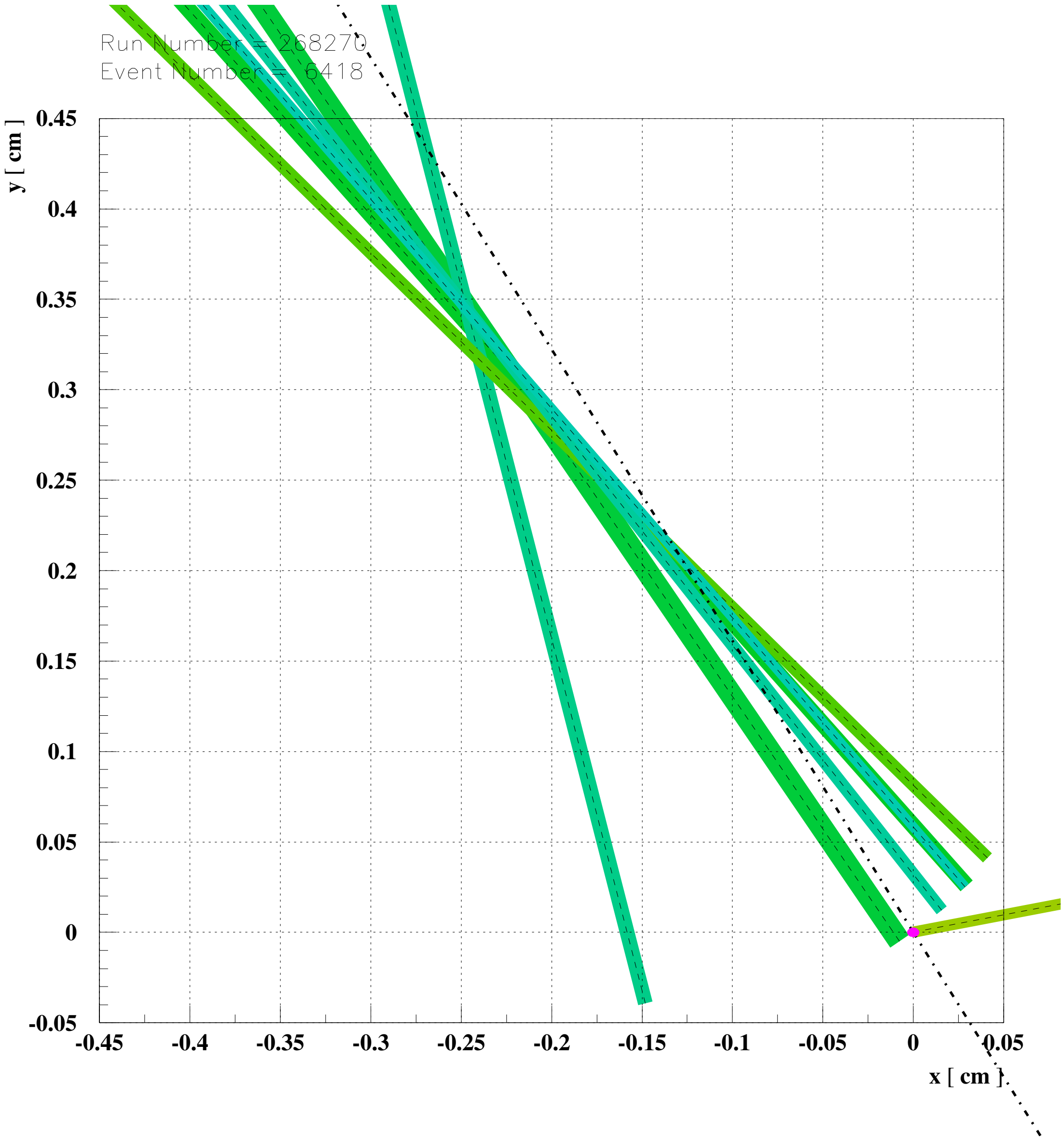

Figure 12: A display of an example data event showing the reconstructed tracks around the primary vertex position in the $x-y$ plane . The primary vertex position is at $x=y=0$. The jet axis is shown by the dash-dotted line. The tracks are shown by dashed lines, with the bands indicating the errors. This event shows a clear interection of tracks at about 4 mm from the primary vertex, giving good evidence for a secondary vertex formed by long lived heavy quark hadrons. This event has $S_2=7.2$.

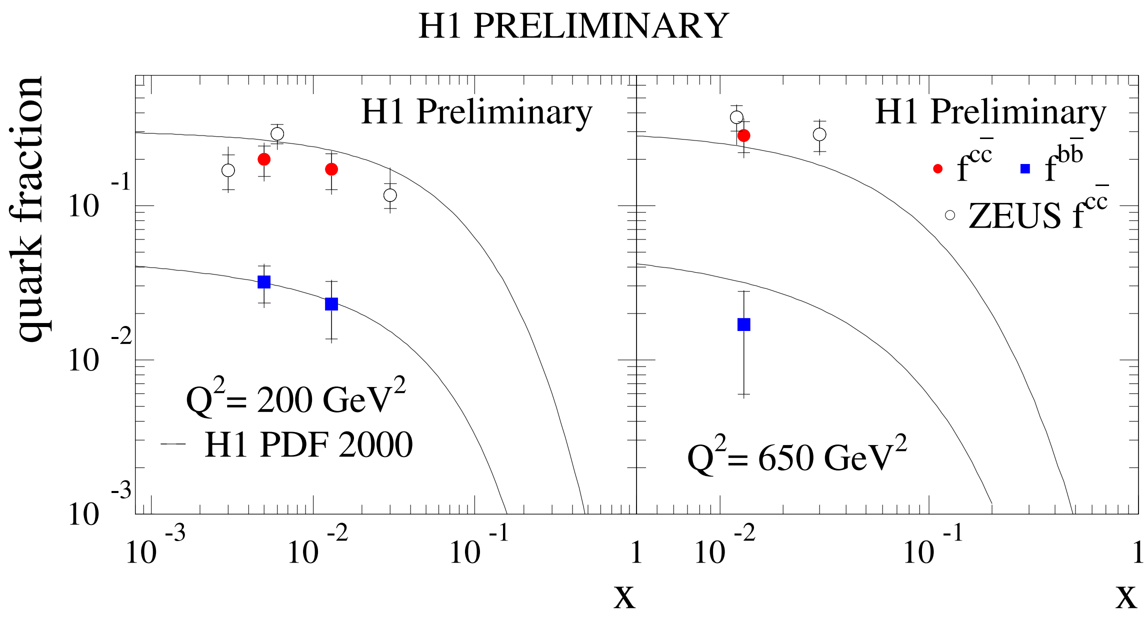

Figure 13: The ratio $f^{c\bar{c}} = F_2^{c\bar{c}}/F_2$ and $f^{b\bar{b}} = F_2^{b\bar{b}}/F_2$ shown as a function of x for 2 different Q^2 values. Also shown is a prediction of the next to leading order QCD fit which was obtained using inclusive cross sections from H1 [1].

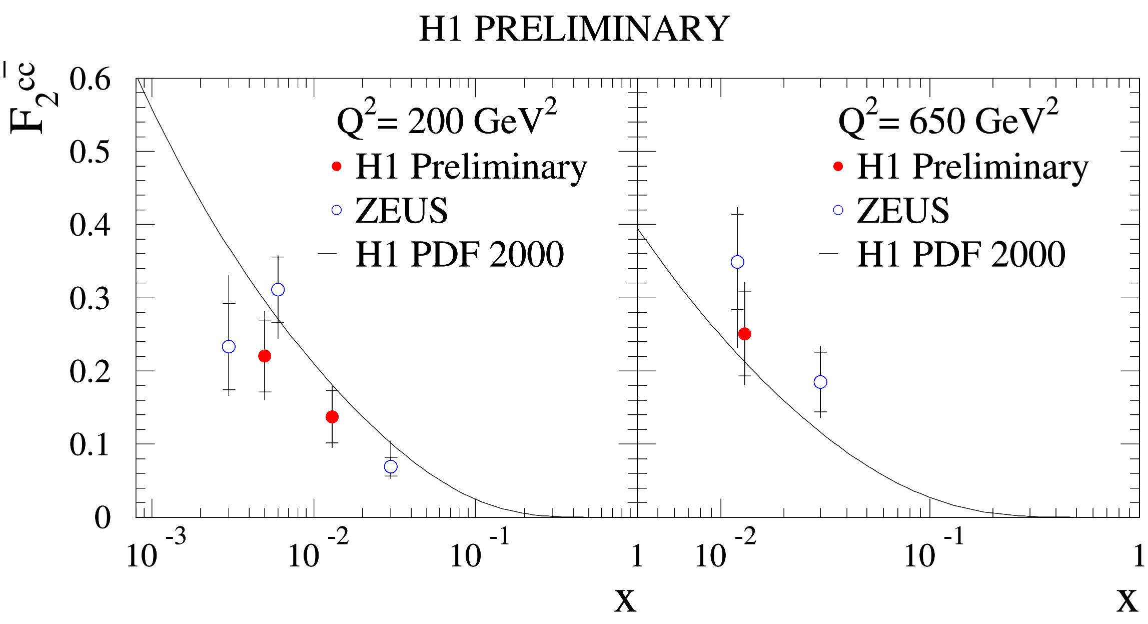

Figure 14: The measured $F_2^{c\bar{c}}$ shown as a function of x for 2 different Q^2 values. Also shown is a prediction of the next to leading order QCD fit which was obtained using inclusive cross sections from H1 [1].

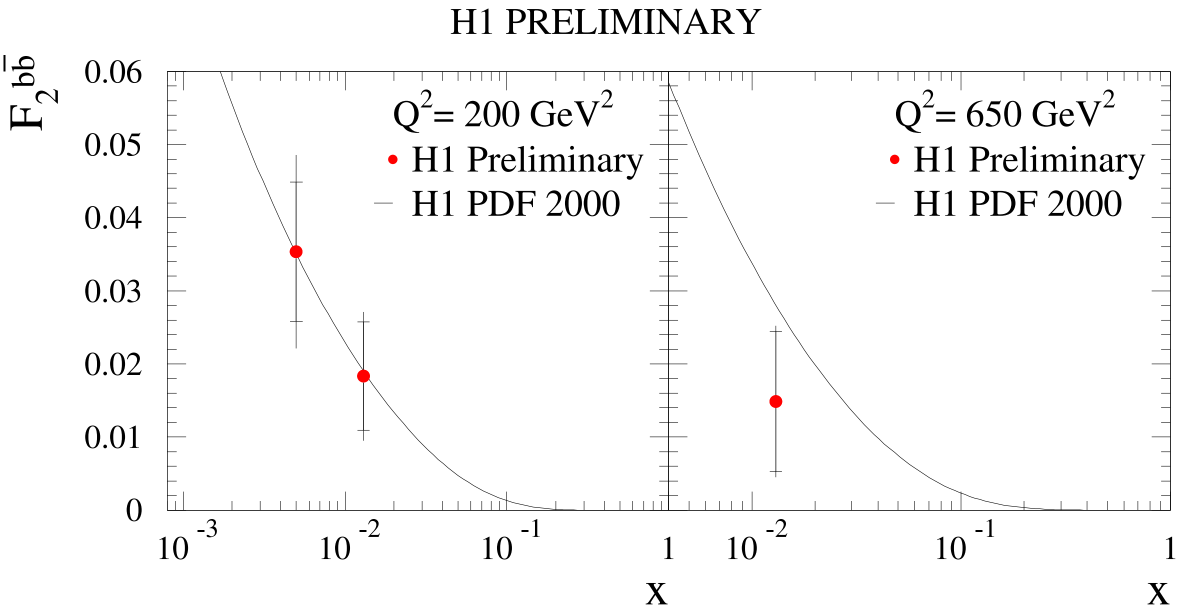

Figure 15: The measured $F_2^{b\bar{b}}$ shown as a function of x for 2 different Q^2 values. Also shown is a prediction of the next to leading order QCD fit which was obtained using inclusive cross sections from H1 [1].